Chandra Multiwavelength Project (ChaMP)
X-ray Point Source Catalog

Minsun Kim, Dong-Woo Kim, Wayne A. Barkhouse, Nancy R. Evans, Paul J. Green, Eunhyeuk Kim, Myung-Gyoon Lee, Amy E. Mossman, John D. Silverman, Harvey D. Tananbaum, Belinda J. Wilkes, and ChaMP collaboration

Harvard-Smithsonian Center for Astrophysics, Smithsonian Astrophysical Observatory
60 Garden Street, Cambridge, MA, USA, mkim@cfa.harvard.edu

http://hea-www.harvard.edu/CHAMP

Abstract

We present the *Chandra* Multiwavelength Projects (ChaMP) X-ray point source catalog with ~6,800 X-ray sources detected in 149 *Chandra* observations covering ~10deg^2. The Full ChaMP catalog sample is seven times larger than the initial ChaMP catalog (Kim, D.-W., et al. 2004, ApJS, 150, 19). The exposure time of our sample ranges up to ~120 *ksec*, corresponding to a X-ray flux limit of $f_{0.5-8.0}$=9x10^{-16} erg sec^{-1} cm^{-2}. The ChaMP x-ray data have been uniformly reduced and analyzed with ChaMP-specific pipelines, and then carefully validated by visual inspection. Our ChaMP catalog includes X-ray photometric data in 8 different energy bands as well as X-ray spectral hardness ratio and colors.

To best utilize the ChaMP catalog, we also present the source reliability, detection probability and positional uncertainty. To quantitatively assess those parameters, we have performed extensive simulations. In particular, we present a set of empirical equations in a few interesting confidence levels: the flux limit as a function of effective exposure time, and the positional uncertainty as a function of source counts and of off-axis angle. The false source detection rate is ~1% of total detected ChaMP sources, while the detection probability is better than ~95% for an source with >50 counts. The typical RMS positional difference between ChaMP X-ray source and *SDSS* optical counterparts is 0.7±0.4" from ~900 matched sources.

Data and Analysis

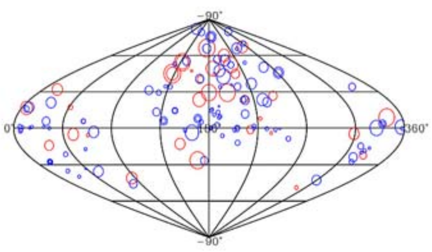

The full ChaMP X-ray point source catalog includes ~6,800 X-ray sources of 149 *Chandra* fields. The location of 149 ChaMP fields are plotted in the left figure.

The ChaMP sources were reduced by a ChaMP-specific pipeline, XPIPE. The XPIPE uses *wavdetect (http://cxc.harvard.edu/ciao)* detections as an input and measures source properties by *xapphot (Kim, E. in preparation)* within a given aperture appropriate for the local PSF (a 95% encircled energy radius at 1.5keV).

Number Distributions

The number distributions of ChaMP X-ray point sources as a function of count, flux, effective exposure time, and off axis angle are displayed in following figures, respectively. The solid line histograms were generated by using all sources, and shaded histograms by using sources having signal to noise ratio of S/N>2.0. The solid and dashed vertical lines indicate the medians of solid line and shaded histograms, respectively.

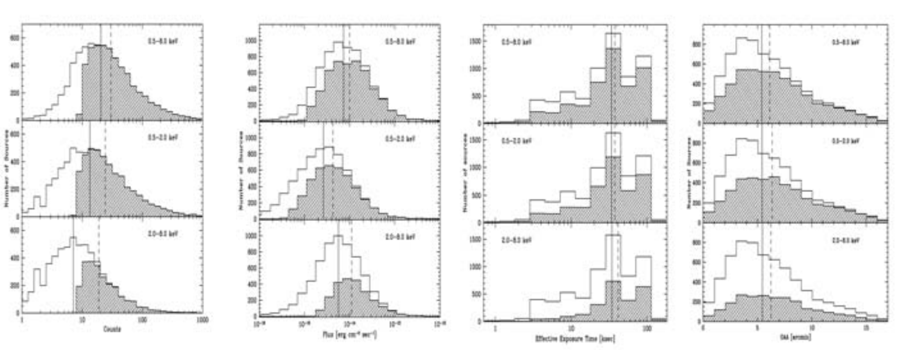

X-ray Color-Color Diagrams

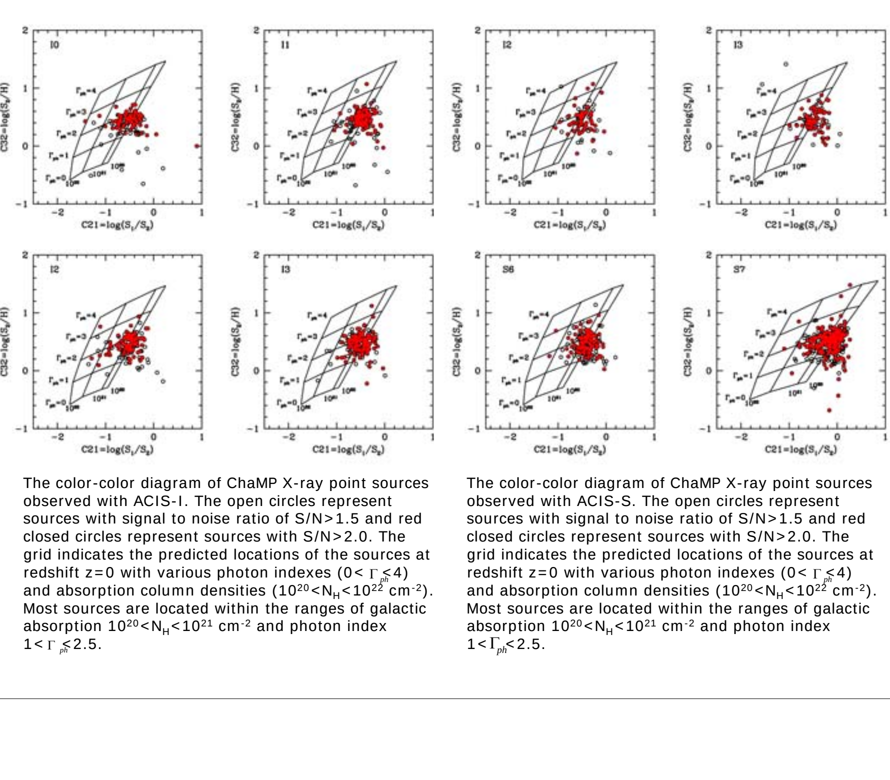

The color-color diagram of ChaMP X-ray point sources observed with ACIS-I. The open circles represent sources with signal to noise ratio of S/N>1.5 and red closed circles represent sources with S/N>2.0. The grid indicates the predicted locations of the sources at redshift z=0 with various photon indexes (0< Γ_{ph}≤4) and absorption column densities (10^{20}<N_H<10^{22} cm^{-2}). Most sources are located within the ranges of galactic absorption 10^{20}<N_H<10^{21} cm^{-2} and photon index 1<Γ_{ph}≤2.5.

The color-color diagram of ChaMP X-ray point sources observed with ACIS-S. The open circles represent sources with signal to noise ratio of S/N>1.5 and red closed circles represent sources with S/N>2.0. The grid indicates the predicted locations of the sources at redshift z=0 with various photon indexes (0< Γ_{ph}≤4) and absorption column densities (10^{20}<N_H<10^{22} cm^{-2}). Most sources are located within the ranges of galactic absorption 10^{20}<N_H<10^{21} cm^{-2} and photon index 1<Γ_{ph}<2.5.

ChaMP Simulations

To characterize the sensitivity, completeness, and positional uncertainty of ChaMP fields, we have performed a series of simulations.

Simulation Process

1. Generate artificial X-ray sources with MARX (http://space.mit.edu/CXC/MARX)
2. Add artificial X-ray sources to the real observed image
3. Detect artificial X-ray sources with *wavdetect*
4. Extract artificial X-ray source properties with *xapphot*
5. Compare input and output artificial X-ray source properties

Assumptions and Ingredients

1. Power law number counts distribution with a slope of -1
2. Power law energy distribution with Γ_{ph} and the Galactic absorption N_H
3. ~13,000 artificial X-ray sources per deg^2
4. Randomly selected the flux from (1) in range of f = 5x10^{-16} ~ 5x10^{-10} [erg cm^{-2} sec^{-1}] in B band, and randomly selected positions of artificial X-ray sources

Count Recovery & Detection Probability

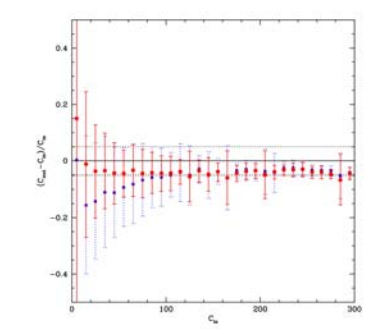

The count recovery rate defined as the ratio of the difference between input and measured output counts to input counts for the artificial X-ray point sources as a function of input counts. The red closed and blue closed squares represent the count recovery rate by *xapphot* and *wavdetect*. Both *xapphot* and *wavdetect* recover well the true counts, however, in the source count range of fainter than ~50, *wavdetect* recovers only ~87% level of true counts while *xapphot* ~96%. Note that Eddington bias is visible in the first positions of both wavdetect and xapphot count recovery rate.

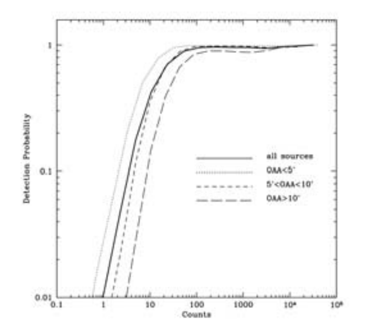

The detection probability of the ChaMP catalog as a function of B band source counts. The thick solid line represents the detection probability of all sources. The dotted, dashed, and long-dashed lines denote the detection probability of sources located at the off axis angle, OAA<5', 5'<OAA<10', and OAA>10', respectively. As expected, the detection probability decreases as the off axis angle OAA increases.

False source Detection Rate

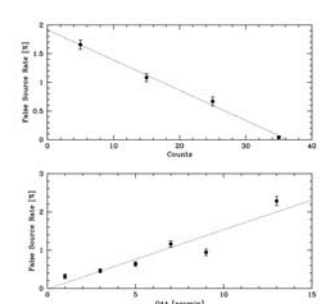

The false source detection rate in the B band extracted by *wavdetect* as a function of source counts (*top*) and off axis angle OAA (*bottom*). ~1% of total detected sources are spurious sources and 80% of spurious sources have counts less than ~30. The false source detection rate increases as the source counts decrease and as the off axis angle increases. The dashed lines indicate the best linear least square fitting results.

$$FSR(Count) = -0.05(\pm0.00)C + 1.92(\pm0.04)$$
$$FSR(OAA) = 0.15(\pm0.02)OAA - 0.01(\pm0.18)$$

Equation of Positional Uncertainty

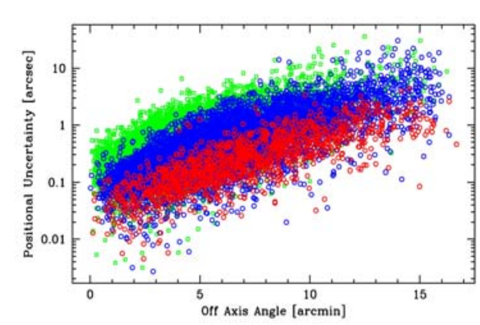

The positional uncertainty of the artificial X-ray sources in three source count ranges as a function of off axis angle. The green, blue, and red symbols represent the positional offset of artificial X-ray sources with count ranges of 0.0<logC<1.2, 1.2<logC<2.0, and logC>2.0, respectively. The counts C are the X-ray source counts extracted by *wavdetect*. It is clearly seen that the positional uncertainty exponentially increases with off axis angle, θ and exponentially decreases as the count, C, increase.

$$LogPU(95\%) = \begin{cases} 0.11\theta - 0.50LogC + 0.19, & \text{when } 0.00 < LogC < 2.14 \\ 0.10\theta - 0.21LogC - 0.43, & \text{when } 2.14 < LogC < 3.30 \end{cases}$$

$$LogPU(90\%) = \begin{cases} 0.11\theta - 0.48LogC + 0.05, & \text{when } 0.00 < LogC < 2.13 \\ 0.10\theta - 0.20LogC - 0.55, & \text{when } 2.13 < LogC < 3.30 \end{cases}$$

$$LogPU(68\%) = \begin{cases} 0.11\theta - 0.46LogC - 0.24, & \text{when } 0.00 < LogC < 2.12 \\ 0.10\theta - 0.19LogC - 0.80, & \text{when } 2.12 < LogC < 3.30 \end{cases}$$

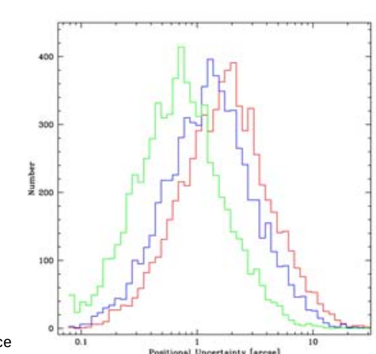

The number distributions of positional uncertainty of ChaMP X-ray point sources estimated from our empirical positional uncertainty equations. Green, blue, and red histogram show the 68%, 90%, and 95% confidence level of positional uncertainty distributions, respectively. The median positional uncertainties are plotted as dotted lines and shown at ~0.7", ~1.3", and ~1.8", respectively.